

SYNTHESIS OF LARGE PLANAR THINNED ARRAYS USING IWO-IFT ALGORITHM

Xinkuan Wang^{*}, Yongchang Jiao, Yan Liu, and Yanyan Tan

Science and Technology on Antenna and Microwave Laboratory, Xidian University, No. 2, South Taibai Road, Xi'an, Shaanxi 710071, China

Abstract—The iterative Fourier technique (IFT) is a high efficiency method that was proposed in recent past for the synthesis of large planar thinned arrays with isotropic radiating elements. However, the selection mechanism of IFT cannot always include the most useful elements in the “turned ON” families, which make the method trap in some local minima. Therefore, in this paper, inspired by invasive weed optimization (IWO) algorithm, a developed version of the iterative Fourier technique (IFT), IWO-IFT, is proposed for thinning large planar arrays. In this new method, the initial weeds are produced by IFT, and are further perturbed by IWO through repeatedly reproduction, dispersion, and exclusion over search space to find better weeds. Numerical results for synthesizing different circular thinned arrays demonstrated the superiority of IWO-IFT over the IFT method.

1. INTRODUCTION

Thinning an array means turning off some elements in a uniformly spaced or periodic array to create a desired amplitude density across the aperture. An element connected to the feed network is “turned ON”, and an element connected to a matched or dummy load is “turned OFF” [1]. There are two advantageous of thinned arrays as compared with periodic filled arrays. Firstly, the number of radiating elements is considerably reduced and hence cut down the array’s cost and weight. Even so, the aperture size is almost maintained, which allows people to get nearly the same resolution of a filled array of equal size. Secondly, thinned arrays present the advantage of easiness of realization, as

Received 20 October 2012, Accepted 7 January 2013, Scheduled 14 January 2013

* Corresponding author: Xinkuan Wang (xkwang@stu.xidian.edu.cn).

different elements usually lie on a regular grid, operate with equal amplitude, and are directly connected to the amplifiers [2]. Owing to the above reasons, thinned arrays designation has become a hot topic in array synthesis area.

Since most of classical optimization methods (including down-hill simplex, Powell's method, and conjugate gradient) are not well suited for thinning arrays, because they can only optimize a few continuous variables and they often get stuck in local minima [3]. Therefore, mainly global optimization approaches, such as genetic algorithm (GA) [1,4], particle swarm optimization (PSO) [5], ant colony optimization (ACO) [6], differential evolution (DE) algorithm [7–9], and some other optimization tools [2,3], were used and shown to be effective for the synthesis of thinned arrays.

In recent years, a high efficiency method, called iterative Fourier technique, has been developed by Keizer. The IFT derives the element excitations from the array factor using successive forward and backward Fourier transforms. The thinning of the array is accomplished by the selecting mechanism of IFT, which involves of forcing the specified number of the element excitations having largest amplitudes equal to a unitary value and the other ones to zero in every iteration cycle. Synthesis results using IFT demonstrated that the thinned linear arrays have lower SLLs than that obtained by GA and PSO [10], and the thinned planar arrays have lower SLLs than that obtained by the statistical density taper approach [11].

According to Equation (1) of [11], the element excitations for thinned arrays is either 1 (turned ON) or 0 (turned OFF), so the array factor is solely decided by the different spatial phases, and these phases are caused by the various spatial positions of turned ON elements. However, because of the randomness of initial element excitations, the selection mechanism of IFT cannot always include the most proper elements in the "turned ON" families. In other words, it is possible that some elements with low excited amplitudes are turned OFF, although they may play an important part in array factor for their spatial phases. Therefore, the method may converge to local solutions.

Owing to the above reason, in this paper, a joint algorithm, IWO-IFT, is proposed to find the array with global minima. In the proposed method, a recently developed algorithm, invasive weed optimization (IWO) [13], is used to perturb the ranking of the amplitudes of the best element excitations for the thinned array produced by IFT in order to find better solutions. Synthesis results for thinning circular arrays with a wide range of diameters validated the superiority of the IWO-IFT.

2. DESCRIPTION OF THE IWO-IFT METHOD

For a planar array with isotropic elements arranged in a square grid at a distance d along M columns and N rows, the array factor AF can be written as [11]

$$AF(u, v) = \sum_{m=0}^{M-1} \sum_{n=0}^{N-1} A_{mn} e^{jkd(mu+nv)} \tag{1}$$

where A_{mn} ($m = 1, 2, \dots, M, n = 1, 2, \dots, N$) is the element excitation located in (m, n) ; A_{mn} is 1 if the element is turned ON and 0 if it is turned OFF; k is the wave number; d is the element spacing; $u = \sin(\theta) \cos(\phi)$ and $v = \sin(\theta) \sin(\phi)$ are the direction cosines; θ, ϕ are elevation and azimuth angles respectively. It could be seen from (1) that all the element excitations constitute a $M \times N$ vector. For convenience, the vector is labeled as $\{A_{mn}\}$. Equation (1) indicates that the element excitations $\{A_{mn}\}$ relate the array factor AF through a finite double fourier series.

To illustrate the process of the IFT method, Figure 1 gives an arbitrary normalized far field pattern with its sampling points in sidelobe region labeled as “circular ring”. The upper dot line in the figure represents the required SLL, and its value is obtained by trial and error [10]. The bottom dot line represents the specified SLL with its value several dBs below the required SLL.

According to Figure 1, in every iteration cycle of the IFT method, AF is obtained by applying 2D-IFFT to $\{A_{mn}\}$. If there are any sampling points whose SLLs surpass the required SLL in the sidelobe

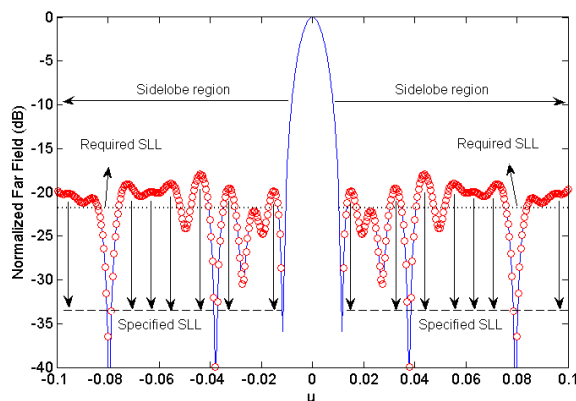


Figure 1. An arbitrary normalized far field pattern to illustrate the IFT.

region of AF , replace their values by the specified SLL. Then, perform 2D-FFT to the modified AF in order to yield the renewed $\{A_{mn}\}$, and truncate $\{A_{mn}\}$ to couple with the array aperture. Finally, sort the amplitudes of $\{A_{mn}\}$ in descending order and perform the selection mechanism to get the thinned array. However, the selection mechanism for IFT may not ensure getting the global solutions, as that is related above.

Inspired from the behavior of colonization of invasive weeds in nature that try to find a suitable place for growth and reproduction, the invasive weed optimization was first proposed by Mehrabian and Lucas for solving continuous optimization problems [12], has found several applications in antenna design [13–17] as well as array’s far field pattern synthesis [18–23]. All the attempts have shown the robustness, high efficiency of the IWO. One of the most notable characteristic of IWO is to find a new seed through a series of normally distributed random numbers with their mean equal to the initial seed and the variance equal to a varying standard deviation. The feature provides a simple way to perturb the ranking of the amplitudes of element excitations obtained by IFT in order to get the arrays with lower SLLs. Therefore, in the IWO-IFT method, the initial population is produced by IFT. To depict the weed in the population, we suppose the best element excitations in an arbitrary trial of IFT can be depicted as $\{A_{mn}^{best}\}$. These element excitations correspond to the array with minimum SLL within the trial, and can be obtained in step 6) of the IFT in [11]. Then, the weed of IWO-IFT can be written as the normalized amplitudes of $\{A_{mn}^{best}\}$

$$\{S_{mn}\} = \{|A_{mn}^{best}\} / \max(\{|A_{mn}^{best}\}) \quad (2)$$

where the vector member S_{mn} represents the normalized amplitude of the element excitation located in (m, n) . According to [11], the element distribution of thinned array is solely decided by $\{S_{mn}\}$, and whether a radiating element is turned ON or turned OFF is decided by the ranking of S_{mn} and the array’s fill factor. Therefore, in the next part of the IWO-IFT, each weed in the population is perturbed by IWO in order to change the ranking of S_{mn} , and in the last part of the method, the selection mechanism of IFT is applied to the renewed $\{S_{mn}\}$. As a result, some formerly “turned OFF” elements can be “turned ON” and vice versa so that better element distribution may be obtained. Moreover, if some vector members are negative in $\{S_{mn}\}$ when performing IWO-IFT, force their values to zero. Figure 2 gives the flow chart of the IWO-IFT method, where T represents the number of turned ON elements, P_{\max} the maximum number of weeds in the population, $iter_{\max}$ the maximum number of iterations. The fitness value in the method is actually the SLL of the thinned array. fit_{worst}

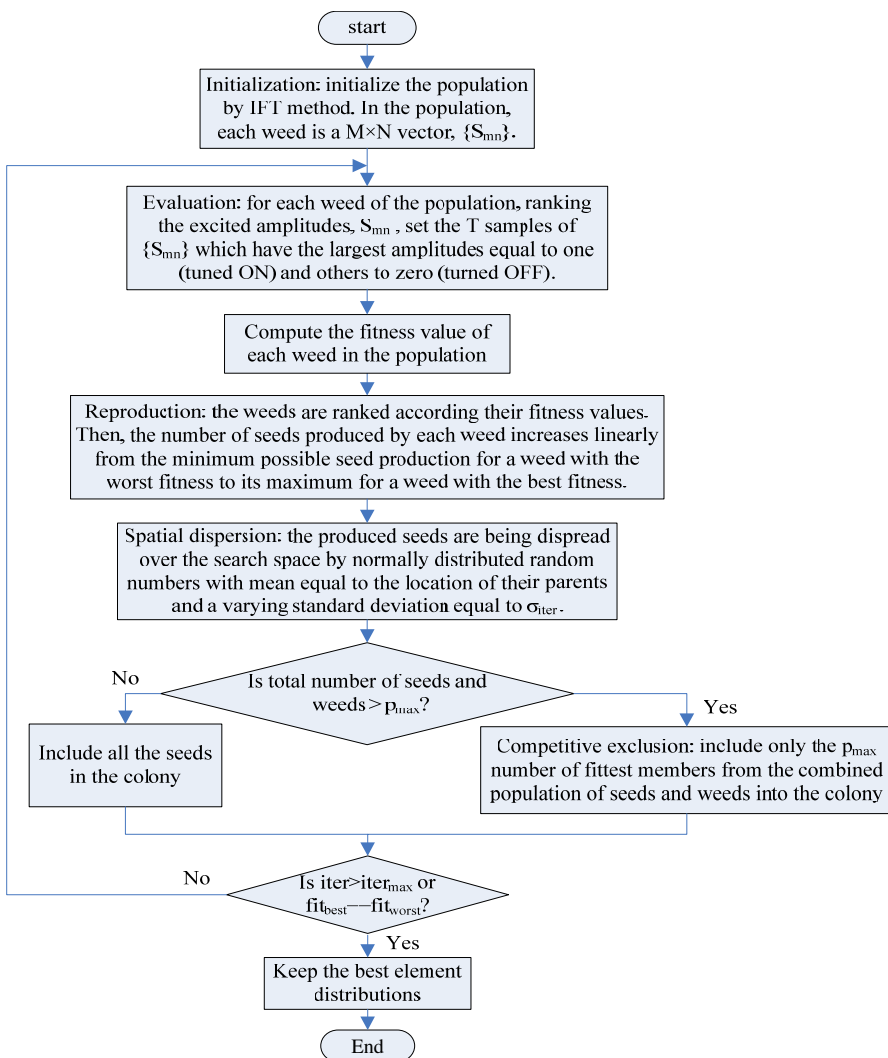


Figure 2. The flow chart showing the IWO-IFT algorithm.

represents the colony’s worst fitness, which corresponds to the weed having maximum SLL in a population. Similarly, fit_{best} represents the best fitness that corresponds to the weed with minimum SLL. When fit_{best} is equal to fit_{worst} , or the number of iterations exceeds $iter_{max}$, the method would be terminated and the best element distribution is kept.

The number of seeds produced by each weed in the population depends on the individual’s fitness value or the ranking of the weed,

and is linearly increased from the minimum number of seeds, s_{\min} , to its maximum value, s_{\max} , then it can be written as

$$N_{seed} = \begin{cases} \text{round}\{[(s_{\max} - s_{\min}) \cdot \text{fit} + s_{\min} \cdot \text{fit}_{best} - s_{\max} \cdot \text{fit}_{worst}] / (\text{fit}_{best} - \text{fit}_{worst})\} \\ \text{s.t. } \text{fit}_{best} \neq \text{fit}_{worst} \end{cases} \quad (3)$$

where fit represents the fitness value of current weed, and round means to round the value in the bracket to its nearest integer. Equation (3) indicates that the weed having better fitness value is more adapted to the colony and thereby produces more seeds.

The varying standard deviation in IWO-IFT can be written as [21]

$$\sigma_{iter} = \begin{cases} \frac{(\text{iter}_{\max} - \text{iter})^3}{(\text{iter}_{\max})^{pow}} (\sigma_{initial} - \sigma_{final}) + \sigma_{final} \\ \text{s.t. } \text{iter} = 0, 1, \dots, \text{iter}_{\max} \end{cases} \quad (4)$$

where iter is the current number of iterations, and $\sigma_{initial}$ and σ_{final} represent the initial and final standard deviations, respectively. The initial value of iter is 0, so when the method arrives at iter_{\max} , the actual number of iterations is $\text{iter}_{\max} + 1$, not iter_{\max} .

3. NUMERICAL EXAMPLES

To illustrate the effectiveness of the proposed method, the IWO-IFT is applied to a wide range of circular arrays with diameters ranging from 25λ to 133.33λ in order to get the array with low SLL, where λ represents the wavelength. Among all the numerical examples, the array element positions are arranged along a square grid 0.5λ apart and the coupling effect between the elements is neglected. The number of sampling points for forward and inverse 2D-FFTs is $K \times K$. In this paper, the initial value of K is 1024 for all the arrays. However, a low value of K could make some points of array factor having high SLLs lost and thus is not enough to depict the full picture of the far field pattern. Therefore, after the best element distribution is obtained at the end of the IWO-IFT, K is further increased to 2048, and 2-D IFFT is applied to the obtained element distribution in order to produce the far field pattern with high resolution. The SLL under this high resolution is deemed as the array's actual SLL. Table 1 gives the assignment values for the involved parameters in IWO-IFT, where N_0 represents the size of initial population.

For a circular thinned array with diameter of 25λ , there are 1928 element positions with 772 elements turned ON due to a 40% fill factor. The optimum thinned array using IWO-IFT has SLL -27.13 dB, about

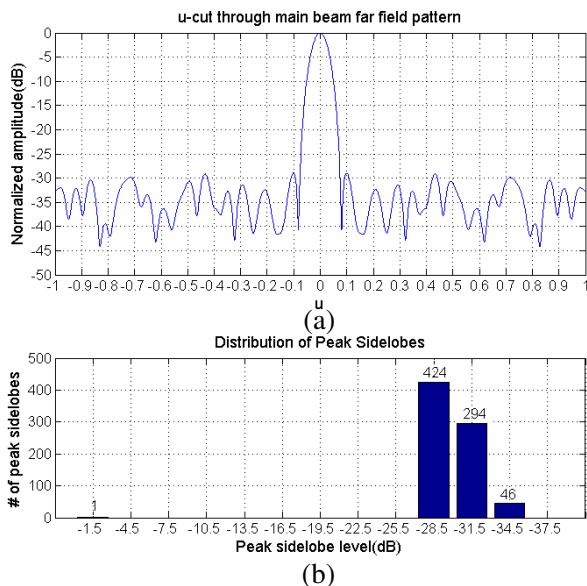


Figure 3. Computed far field pattern of the 25λ circular thinned array with a 40% fill factor. (a) Principal u-cut. (b) PSL distribution of whole visible space of the far field.

Table 1. The involved parameter values in IWO-IFT.

Symbol	N_0	$iter_{max}$	P_{max}	s_{max}	s_{min}	$\sigma_{initial}$	σ_{final}
Value	50	20	250	5	1	0.3	10^{-3}

0.7 dB below the report in [11]. Figure 3(a) shows the principal u-cut of the array’s far field pattern going through the main beam peak. Figure 3(b) the histogram depicts the peak level distributions of all 765 sidelobes (include mainlobe) of the array pattern located in visible space, and the visible space satisfies the relation

$$u^2 + v^2 \leq 1 \tag{5}$$

For the same thinned array, the convergence curves in Figure 4 respectively depict the best, the worst and the mean fitness value in the colony that changed with the number of iterations. They indicate that at the beginning of the iteration, the individual differences in the colony are evident. The best, the worst and the mean fitness value at iteration #0 is -26.47 dB, -19.99 dB, and -23.16 dB respectively. However, the differences between the three fitness values are narrowed with the increment of iterations, and the three fitness values converged

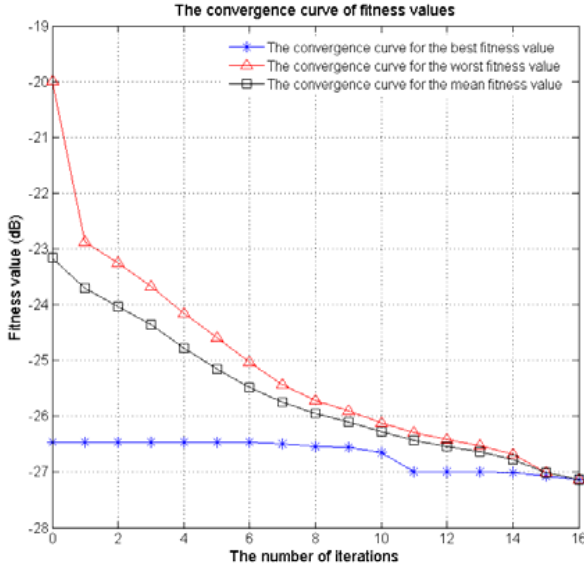


Figure 4. The convergence curves of different fitness values in the colony for synthesis of the 25λ circular thinned array that has a 40% fill factor.

to the same point, -27.14 dB at the iteration #16. Then, the method is terminated, and the individual with best fitness value at iteration #16 is deemed as the optimum element distribution. One may have a question that why the best fitness value is slightly lower than the value given in Figure 3(a) (-27.13 dB). The reason is that the size of sampling points is small (K is 1024) in the course of the IWO-IFT, which makes some points having high SLLs lost. Therefore, at the end of the IWO-IFT, the actual SLL of the same thinned array is rechecked by doubling the size of sampling points of 2D-IFFT to produce the far field pattern with high resolution.

For a circular array with diameter of 50λ and that is 30% filled, Figure 5 depicts its element distribution across the aperture obtained by IWO-IFT, where the turned ON elements are labeled as “crosses”. The SLL of the far field pattern produced by this element distribution is -31.03 dB, which is about 0.5 dB lower than the published report by IFT [11]. Furthermore, Figure 6 depicts the thinning result for the array having 100λ diameter and a 40% fill factor. The principle u-cut of the array’s far field pattern as shown in Figure 6(a), has SLL -35.3 dB. The value is about 2.6 dB lower than the published report by IFT [11]. Figure 6(b) depicts the peak SLL distributions of the array’s far field pattern located in visible space. Figure 7 the convergence

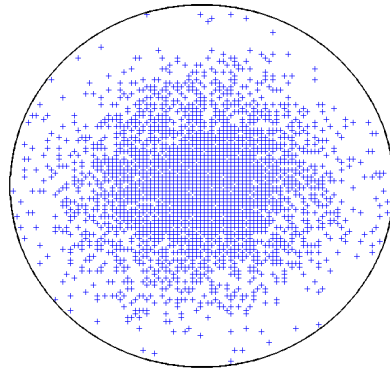


Figure 5. Location of the 2337 turned ON elements for the 50λ circular array having a 30% fill factor.

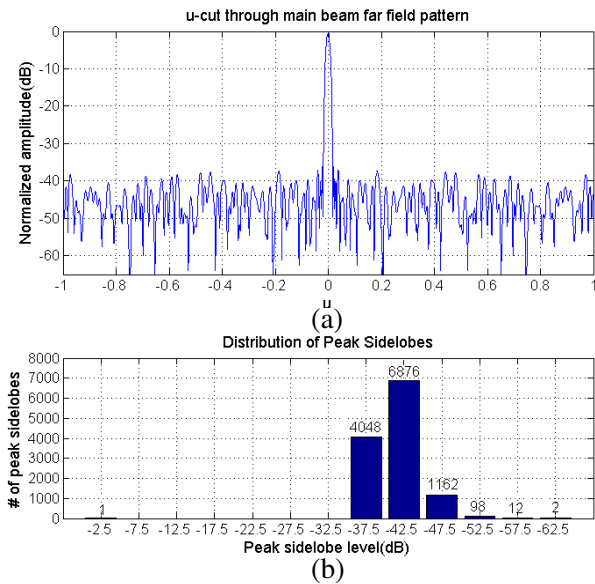


Figure 6. Computed far field pattern of the 100λ circular thinned array with 40% fill factor. (a) Principal u-cut. (b) PSL distribution of whole visible space of the far field.

curves of the best, worst, and mean fitness values indicate that the population evolution is terminated at iteration #20, where there are little differences between the three fitness values. The distribution of the 12514 turned ON elements for this thinned array is depicted in Figure 8.

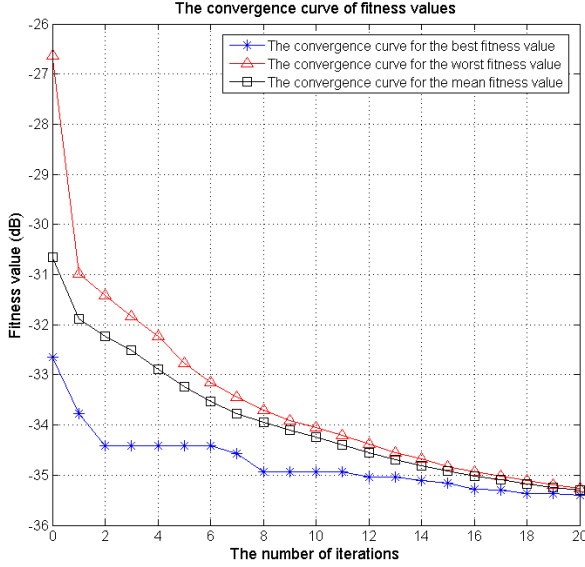


Figure 7. The convergence curves of different fitness values in the colony for synthesis of the 100λ circular thinned array that has a 40% fill factor.

Table 2. The comparative results using IWO-IFT and IFT for the synthesis of different circular arrays.

Diameter (λ)	T	f (%)	SLL (dB)		Directivity (dB)		3 dB Beamwidth (Δu)	
			IWO-IFT	IFT	IFT-IWO	IFT	IWO-IFT	IFT
25	578	30.0	-25.93	-25.5 [11]	31.79	31.8 [11]	0.0692	0.0648 [1]
	772	40.0	-27.13	-26.4 [11]	32.92	33.0 [11]	0.058	0.0549 [11]
	964	50.0	-27.77	-27.2 [24]	33.99	33.96 [24]	0.0509	0.0496 [24]
33.33	1031	30.0	-27.87	-27.1 [11]	34.21	34.2 [11]	0.0455	0.0445 [11]
	1374	40.0	-29.17	-28.5 [11]	35.52	35.4 [11]	0.0427	0.0403 [11]
50	2337	30.0	-31.03	-30.5 [11]	37.72	37.8 [11]	0.0322	0.0307 [11]
	3116	40.0	-32.14	-31.8 [11]	39.02	38.9 [11]	0.0269	0.0261 [11]
66.67	4146	30.0	-33.05	-32.6 [11]	40.21	40.2 [11]	0.0224	0.0227 [11]
	5528	40.0	-33.72	-33.6 [11]	41.45	41.4 [11]	0.0197	0.0197 [11]
100	9386	30.0	-35.54	-35.4 [11]	43.68	43.6 [11]	0.0145	0.0144 [11]
	12514	40.0	-35.30	-32.7 [11]	44.95	45.0 [11]	0.0128	0.0129 [11]
133.33	15021	27.0	-37.22	-36.0 [24]	45.71	45.72 [24]	0.0112	0.0115 [24]

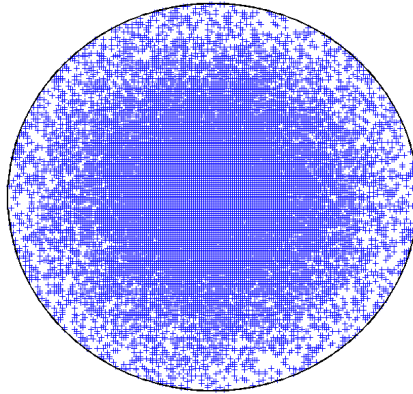


Figure 8. Location of the 12514 turned ON elements for the 100λ circular array having a 40% fill factor.

Table 3. The computational cost for the synthesis of different circular arrays using IFT and IWO-IFT.

Diameter (λ)	T	f (%)	IFT		IWO-IFT	
			Computational cost (hours)	SLL (dB)	Computational cost (hours)	SLL (dB)
25	578	30.0	2.98	-25.51	2.25	-25.93
	772	40.0	2.33	-26.64	2.28	-27.13
	964	50.0	2.00	-27.41	2.24	-27.77
33.33	1031	30.0	2.54	-27.25	2.62	-27.87
	1374	40.0	2.27	-28.80	2.72	-29.17
50	2337	30.0	2.61	-30.31	2.73	-31.03
	3116	40.0	2.55	-31.58	2.45	-32.14
66.67	4146	30.0	2.61	-32.62	2.64	-33.05
	5528	40.0	3.05	-33.20	2.54	-33.72
100	9386	30.0	3.78	-35.42	2.71	-35.54
	12514	40.0	3.85	-32.83	3.09	-35.30
133.33	15021	27.0	4.92	-36.16	3.07	-37.22

Table 2 gives the comparative results using IWO-IFT and IFT for the synthesis of circular arrays with different diameters, where f represents the fill factor. It demonstrated that for all the considered illustrations, the thinned arrays obtained by IWO-IFT have lower SLLs than that obtained by IFT, and this phenomenon become more evident for the arrays with diameter of 100λ and 133.33λ . All the results in this paper were obtained by a PC equipped with an Intel Pentium Dual core E5200 Processor and 2 GB RAM. The runtime for all the thinned arrays ranges from 2 hours to 3 hours.

One may say that more trials of IFT may facilitate producing the array with lower SLLs, because the results in [11] is obtained by performing IFT only 50 trials. However, the improvement can be neglected. For example, we suppose the number of trials for each selected array is 500, Table 3 gives the SLL results and the computational cost for synthesizing similar arrays as is depicted in Table 2. It could be seen from Table 3 that the quality of solutions is almost not improved comparing with the results in [11], and the computational burden is similar to IWO-IFT. In fact, when performing the IFT for each selected array in Table 2 2000 trials regardless of the considerable computational cost, the solutions quality is also not improved. Some results in Table 3 are not better than that in [11], because different RSSLs have been adopted, and we do not know the values of RSSL for most thinned arrays in [11].

4. CONCLUSION

A joint algorithm, IWO-IFT, is proposed for the synthesis of large planar thinned arrays. In the proposed method, the initial weeds are produced by IFT. Then, the weeds are perturbed by IWO in order to find better weeds through changing the ranking of the amplitudes of the element excitations. Simulation results validated the superiority of the proposed method to IFT in terms of getting the arrays with lower SLLs. Furthermore, by a small modification, the method can also be applied to synthesize linear thinned arrays.

REFERENCES

1. Haupt, R. L., "Thinned arrays using genetic algorithms," *IEEE Trans. on Antennas and Propag.*, Vol. 42, 993–999, 1994.
2. Bucci, O. M., T. Isernia, and A. F. Morabito, "A deterministic approach to the synthesis of pencil beams through planar thinned arrays," *Progress In Electromagnetics Research*, Vol. 101, 217–230, 2010.

3. Fernández-Delgado, M., J. A. Rodríguez-González, R. Iglesias, S. Barro, and F. J. Ares-Pena, "Fast array thinning using global optimization methods," *Journal of Electromagnetic Waves and Applications*, Vol. 24, No. 16, 2259–2271, 2010.
4. Mahanti, G. K., N. N. Pathak, and P. K. Mahanti, "Synthesis of thinned linear antenna arrays with fixed sidelobe level using real-coded genetic algorithm," *Progress In Electromagnetics Research*, Vol. 75, 319–328, 2007.
5. Wang, W.-B., Q. Feng, and D. Liu, "Synthesis of thinned linear and planar antenna arrays using binary PSO algorithm," *Progress In Electromagnetics Research*, Vol. 127, 371–387, 2012.
6. Quevedo-Teruel, Ó. and E. Rajo-Iglesias, "Ant colony optimization in thinned array synthesis with minimum sidelobe level," *IEEE Antennas and Wireless Propagation Letters*, Vol. 5, 349–352, 2006.
7. Zhang, L., Y.-C. Jiao, B. Chen, and F.-S. Zhang, "Synthesis of linear aperiodic arrays using a self-adaptive hybrid differential evolution algorithm," *IET Microw. Antennas Propag.*, Vol. 5, 1524–1528, 2011.
8. Ghosh, P. and S. Das, "Synthesis of thinned planar concentric circular antenna arrays — A differential evolutionary approach," *Progress In Electromagnetics Research B*, Vol. 29, 63–82, 2011.
9. Mandal, A., H. Zafar, S. Das, and A. V. Vasilakos, "Efficient circular array synthesis with a memetic differential evolution algorithm," *Progress In Electromagnetics Research B*, Vol. 38, 367–385, 2012.
10. Keizer, W. P. M. N., "Linear array thinning using iterative FFT techniques," *IEEE Trans. on Antennas and Propag.*, Vol. 56, 2757–2760, 2008.
11. Keizer, W. P. M. N., "Large planar array thinning using iterative FFT techniques," *IEEE Trans. on Antennas and Propag.*, Vol. 57, 3359–3362, 2009.
12. Mehrabian, A. R. and C. Lucas, "A novel numerical optimization algorithm inspired from weed colonization," *Ecological Informatics*, Vol. 1, 355–366, 2006.
13. Dadalipour, B., A. R. Mallahzadeh, and Z. Davoodi-Rad, "Application of the invasive weed optimization technique for antenna configurations," *IEEE Antennas and Propagation Conference*, 425–428, Loughborough, March 2008.
14. Mallahzadeh, A. R., S. Es'haghi, and H. R. Hassani, "Compact U-array MIMO antenna designs using IWO algorithm," *Interna-*

- tional Journal of RF and Microwave Computer-aided Engineering*, 568–576, 2009.
15. Sedighy, S. H., A. R. Mallahzadeh, M. Soleimani, and J. Rashed-Mohassel, “Optimization of printed Yagi antenna using invasive weed optimization (IWO),” *IEEE Antennas and Wireless Propagation Letters*, Vol. 9, 1275–1278, 2010.
 16. Monavar, F. M. and N. Komjani, “Bandwidth enhancement of microstrip patch antenna using Jerusalem cross-shaped frequency selective surfaces by invasive weed optimization approach,” *Progress In Electromagnetics Research*, Vol. 121, 103–120, 2011.
 17. Monavar, F. M., N. Komjani, and P. Mousavi, “Application of invasive weed optimization to design a broadband patch antenna with symmetric radiation pattern,” *IEEE Antennas and Wireless Propagation Letters*, Vol. 10, 1369–1372, 2011.
 18. Roshanaei, M., C. Lucas, and A. R. Mehrabian, “Adaptive beamforming using a novel numerical optimization algorithm,” *IET Microw. Antennas Propag.*, Vol. 3, 765–773, 2009.
 19. Pal, S., A. Basak, S. Das, and A. Abraham, “Linear antenna array synthesis with invasive weed optimization algorithm,” *IEEE International Conference of Soft Computing and Pattern Recognition*, 161–166, 2009.
 20. Karimkashi, S. and A. A. Kishk, “Invasive weed optimization and its features in electromagnetics,” *IEEE Trans. on Antennas and Propag.*, Vol. 58, 1269–1278, 2010.
 21. Basak, A., S. Pal, S. Das, A. Abraham, and V. Snasel, “A modified invasive weed optimization algorithm for time-modulated linear antenna array synthesis,” *IEEE Congress on Evolutionary Computation*, 1–8, 2010.
 22. Roy, G. G., S. Das, P. Chakraborty, and P. N. Suganthan, “Design of non-uniform circular antenna arrays using a modified invasive weed optimization algorithm,” *IEEE Trans. on Antennas and Propag.*, Vol. 59, 110–118, 2011.
 23. Zaharis, Z. D., C. Skeberis, and T. D. Xenos, “Improved antenna array adaptive beam-forming with low side lobe level using a novel adaptive invasive weed optimization method,” *Progress In Electromagnetics Research*, Vol. 124, 137–150, 2012.
 24. Keizer, W. P. M. N., “Amplitude-only low sidelobe synthesis for large thinned circular array antennas,” *IEEE Trans. on Antennas and Propag.*, Vol. 60, 1157–1161, 2012.